IEEE Access
Multidisciplinary | Rapid Review | Open Access Journal

Received October 23, 2019, accepted November 4, 2019, date of publication November 8, 2019, date of current version December 2, 2019.

Digital Object Identifier 10.1109/ACCESS.2019.2952386

Simultaneous Robust Control and Sensor Fault Detection for a Ducted Coaxial-Rotor UAV

CHANG XU[1,2], HONGGUANG JIA[1,3], AND ZAIBIN CHEN[1,2]

[1]Changchun Institute of Optics, Fine Mechanics and Physics, Chinese Academy of Sciences, Changchun 130033, China
[2]Department of Mechanical Manufacturing and Automation, University of Chinese Academy of Sciences, Beijing 100049, China
[3]Chang Guang Satellite Technology Company, Ltd., Changchun 130033, China

Corresponding author: Chang Xu (13043324363@163.com)

This work was supported in part by the Knowledge Innovation Program of the Chinese Academy of Sciences under Grant YYYJ-1122, and in part by the Science Fund for Young Scholars of the National Natural Science Foundation of China under Grant 61505203.

ABSTRACT This paper addresses the aerodynamic modeling, observer-based state-feedback robust control and sensor fault detection for a laboratory ducted coaxial-rotor UAV (DCUAV). First, by introducing the main model elements of this novel unmanned vehicle, the detailed nonlinear mathematical model of the hovering flight UAV is presented. Second, through introducing a weighting matrix and a new form of change-of-variables, a new method is proposed by designing two different systems simultaneously as detector and controller. An observer-based controller is proposed to achieve the control objective and finite-frequency sensor fault detection objective simultaneously. The observer-based controller design method is derived from a new formulation of linear matrix inequality (LMI), which can achieve the prescribed H_∞ performance, H_- performance and the stability of the closed-loop system. By constructing a new matrix decomposition form, the simultaneous design of detector parameters and controller parameters is solved. Finally, simulations are conducted for the hover flight with disturbances and sensor faults, the results show the satisfactory control performance and fault detection performance.

INDEX TERMS Ducted coaxial rotors, UAV, observer-based, robust control, sensor fault detection, linear matrix inequalities.

I. INTRODUCTION

In recent decades, the development of unmanned aerial vehicles covers a wide range of sizes and capabilities [1]–[4], which has attracted increased interest in developing control algorithms and fault detection methods. Among various UAVs, the ducted coaxial-rotor UAV(DCUAV) is well-suited for a variety of flight missions and complex environments. It is capable of high-speed flight in addition to the hover and vertical take-off and landing capabilities. Compared with traditional helicopter, the ducted coaxial-rotor UAV will produce greater tension than isolated propeller with the same diameter, which makes the fuselage structure more compact [5]–[8]. The configuration layout of the ducted coaxial-rotor UAV developed by our laboratory is depicted in Fig.1. The DCUAV is highly unstable and highly nonlinear with complex aerodynamics, which makes the control of the DCUAV present many unique challenges. Furthermore, any undetected sensor faults may degrade the overall system performance, cause catastrophic accidents, and even threaten flight safety [9], [10]. The main mission of our designed DCUAV is surveying and mapping, it is often equipped with photographic equipment. Therefore, in order to achieve high flight performance and fault diagnosis and fault tolerance performance, it is necessary to design a controller with the capability to solve the simultaneous control and fault detection problem.

In the literature, various control and detection approaches of the ducted fan aircrafts, coaxial-rotor aircrafts and other types of UAVs, have been developed to achieve flight performances and fault detection objective. Reference [11] used a PID control method, which has a simple control structure, but it has a poor adaptability for the coupling between axes. In [6], by comparing PID, LQR and H_∞ mixed synthesis techniques on linearized sub-plants of a small coaxial helicopter about hover, it is proved that the robust H_∞ controller has better performance in suppressing the disturbances caused by the wind. Backstepping techniques have been used in attitude

The associate editor coordinating the review of this manuscript and approving it for publication was Sing Kiong Nguang.

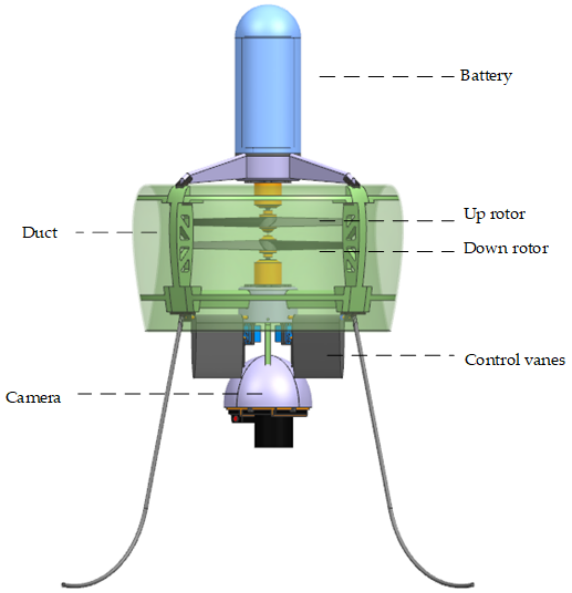

FIGURE 1. Layout of the DCUAV.

stabilization [12] and trajectory tracking [13] for small VTOL UAVs. An extended state observer-based controller is developed for a coaxial-rotor UAV in [14], where the observer is used to estimate the state and the unknown aerodynamic disturbance. The closed-loop system is stabilized by the interaction of the controller and the observer. Nonlinear dynamic inversion control in [15] and sliding mode control in [16] are designed for one ducted-fan UAV, but both rely on the accuracy of the UAV mathematical model. Neural Network techniques are also presented in many literatures. In [17], a controller combined the neural networks and adaptive backstepping control is designed for a ducted-fan UAV. A neural network based optimal controller for an unmanned helicopter was proposed in [18] to accomplish trajectory tracking. However, the disturbances, uncertainties and faults are not fully taken into consideration, and the majority of their methods have limitations in the engineering application.

On the other hand, the sensor faults usually emerge in low-frequency domain in our DCUAV flight practice, which is one of the main causes of aircraft system instability and poor flight performance. This motivates the problem of integrated control and fault detection that has attracted significant attention in recent years. A supertwisting-based observer is utilized to estimate the servo's stuck fault for the tilt trirotor UAV in [48]. Based on the proposed observer, a nonlinear FTC controller is developed to maintain the UAV's attitude stability. In [45], the unknown input observer was used to diagnose the icing and actuator faults of a typical small UAV. In [49], an integrated fault tolerant control framework was proposed based on Reduced-order simultaneous state and fault estimator for discrete-time linear time-invariant systems, which was performed at the H_∞ optimization level. Also, the observer-based fault detection and tracking control method was proposed in [46] and [47] for a quadrotor UAV and a planar vertical take-off and landing UAV respectively. By integrating radial base function neural network (RBFNN) with fuzzy sliding mode control, an actuator fault tolerant control technique for a coaxial octorotor UAV was introduced in [19]. In [20], a structured H_∞ controller tuned by a non-smooth optimization algorithm was proposed for a tandem coaxial ducted fan aircraft. The proposed method can recover the desired performance in the presence of actuator fault, disturbance and system uncertainty. Backstepping technique in [21] and adaptive fault tolerant control in [22] are also presented for quadrotor UAVs. However, little attention has been paid to the fault detection and the detection system is often designed separately form flight control system. Therefore, design of fault tolerant control flight system and faults detection system simultaneously has crucial significance in the field of DCUAV research.

In order to achieve flight control objectives and detect faults simultaneously, especially for systems with uncertainties in model, H_∞ control theories and H_- performance index are widely used [24]–[28]. Since the sensor faults in our UAV flight system usually emerge in low frequency domain, which will make the faults hidden by control actions and difficult to be detected in the early stage [29]. Some finite-frequency fault detector design approaches have been considered in many works by KYP Lemma [30] [31]. With the defined robust performance index and fault sensitivity index, some works have presented the controller and fault detector design as a multi-objective optimization problem [32], [33]. In [34], the simultaneous fault detection and control problem for linear uncertain discrete-time systems has been studied. In [35] and [36], a single unit is designed as detector/controller to produce the detection and control signals. However, by unifying the control and detection units into a single unit, these schemes may not be able to take both control and detection objectives into account. Further, the system model uncertainties are also not taken into consideration.

Motivated by the aforementioned analysis, a new DCUAV integrated control and sensor fault detection methodology considering the system model uncertainties is introduced based on H_∞ theory, H_- index performance and finite-frequency index performance. The main contributions of this paper are summarized as follows. First, the mathematical model of the ducted coaxial-rotor UAV is obtained by analyzing the aerodynamic forces and moments acting on the vehicle. Second, simultaneous control and sensor fault detection problem is considered, by introducing a new linear change-of-variables, the observer-based controller design conditions can convert into convex optimization problem with linear matrix inequalities. Note that, most papers presented the schemes which were designed to implement fault detection and control by a single unit. Therefore, in some cases, considerations cannot be given to both control objective and detection objective. Third, unlike most articles on fault-tolerant control and multi-objective optimization, the proposed method fully considers the parameter

uncertainties of the ducted coaxial-rotor UAV model, rather than simply treating it as unknown disturbances. And this mathematic processing is very meaningful, since the ducted coaxial-rotor UAV has a more complex aerodynamic model. Finally, the strict observer-based controller design condition is developed for guaranteeing the robustness, H_- performance and stability of the flight system in the presence of uncertainties.

This paper is organized as follows: Section 2 presents the dynamical model of the ducted coaxial-rotor UAV. Section 3 considers the simultaneous robust control and sensor fault detection, controller and fault detector design conditions are developed. The simulation results and discussions are presented in Section 4. Finally, the conclusions are provided in Section 5.

Notation: for a matrix A, A^T, $A^\perp$ denote its transpose and orthogonal complement, respectively; denotes I the identity matrix with an appropriate dimension; The Hermitian part of a square matrix A is denoted by $He\,(A) = A+A^T$; The symbol * in a matrix represents the symmetric entries.

II. DYNAMIC MODELING OF DCUAV

In this section, we describe the dynamic model of the ducted coaxial-rotor UAV. Consider the ducted coaxial-rotor UAV depicted in Fig.1 as a solid body incorporating a force and moment generation process. Let $Ox_by_bz_b$ be the body-fixed frame attached to the center of gravity of the UAV, where x_b is the longitudinal axis, y_b is the lateral axis and z_b is the vertical direction, and $Ox_gy_gz_g$ be the Earth frame as depicted in Fig. 2. The position and attitude of the UAV in the body-axes coordinate relative to the earth-axes coordinate are usually described by three Euler angles, where φ is the Roll angle (rotation around the x-axis), θ is the Pitch angle (rotation around the y-axis), and ϕ is the Yaw angle (rotation around the z-axis).According to the principle of coordinate transfer, the transfer matrix (1) between $Ox_gy_gz_g$ and $Ox_by_bz_b$ is obtained, as shown at the bottom of this page. The accurate flight dynamics model of the ducted coaxial rotorcraft can be expressed by the Newton-Euler formalism:

$$\begin{aligned} m\dot{v} + m\,(\omega \times v) &= F \\ J\dot{\omega} + (\omega \times J\omega) &= M \end{aligned} \tag{2}$$

The force and moment vectors can be expressed as:

$$\begin{aligned} F &= F_{grav} + F_{rotor} + F_{vane} + F_{duct} \\ M &= M_{grav} + M_{rotor} + M_{vane} + M_{gyro} \end{aligned} \tag{3}$$

where all the component forces and moments are discussed below.

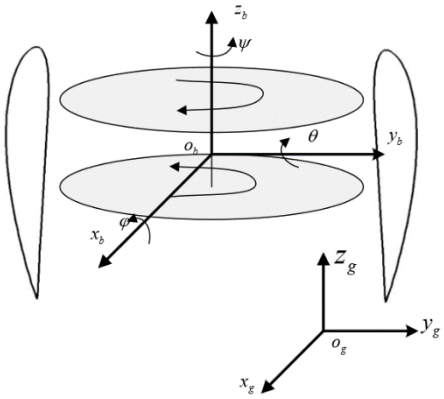

FIGURE 2. Frame system of the DCUAV.

A. GRAVITY

The gravity of the UAV expressed in earth-axes can be as:

$$F_{eg} = \begin{bmatrix} 0 & 0 & mg \end{bmatrix}^T \tag{4}$$

Considering the transformation between the body-axes and the earth-axes, the gravitational force in body-axes coordinate system is given by:

$$F_{grav} = R_{gb}F_{eg} = \begin{bmatrix} mg\cos\varphi\sin\theta \\ -mg\sin\varphi \\ mg\cos\theta\cos\varphi \end{bmatrix} \tag{5}$$

B. COAXIAL-ROTORS

The thrust generated by the coaxial-rotors in the duct can be expressed by the aerodynamic actuator disk theory (Bramwell et al.2001)

$$T_i = \rho C_{T,i} A\,(\omega_i R)^2 \tag{6}$$

where $T_i\,(i = up, dw)$ are thrusts when the rotor blades spin in the opposite direction, ρ is the freestream density, $C_{T,i}$ is the lift coefficient, A is the rotor disk area, ω_i is the angular velocity of the rotor, and R is the radius of the rotor. Since the UAV discussed in this paper uses fixed-pitch rotors, $C_{T,i}$ is constant like the other parameters in (6) expect the variable ω_i. Hence, the force on the vehicle due to the rotor can now be simplified to

$$F_{rotor} = \begin{bmatrix} 0 \\ 0 \\ k_{T,up}\omega_{up}^2 + k_{T,dw}\omega_{dw}^2 \end{bmatrix} \tag{7}$$

with $k_{T,i}$ representing a lumped lift coefficient that needs to be identified. The moments generated by the rotors can apply

$$\begin{aligned} R_{gb}\,(\phi,\theta,\varphi) &= R_x^T\,(\varphi)\,R_y^T\,(\theta)\,R_z^T\,(\phi) \\ &= \begin{bmatrix} \cos\theta\cos\phi & \cos\theta\sin\phi & -\sin\theta \\ \cos\phi\sin\theta\sin\varphi - \sin\phi\cos\varphi & \sin\varphi\sin\theta\sin\phi + \cos\phi\cos\varphi & \cos\theta\sin\phi \\ \cos\phi\sin\theta\cos\varphi + \sin\phi\sin\varphi & \sin\phi\sin\theta\cos\varphi - \cos\phi\sin\varphi & \cos\theta\cos\phi \end{bmatrix} \end{aligned} \tag{1}$$

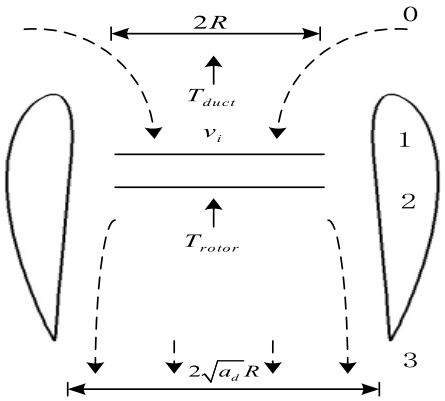

FIGURE 3. Flow schematic diagram.

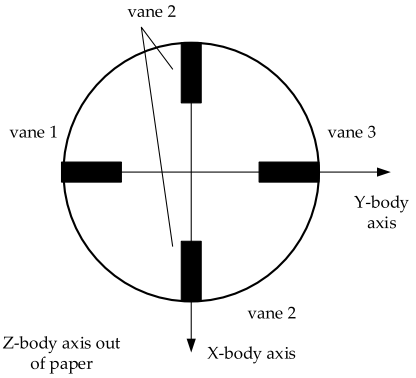

FIGURE 4. Vane configuration for ducted fan as viewed from above.

the similar assumptions and formulations above to establish the relationship with the angular velocity of the rotor:

$$M_{rotor} = k_{M,i}\omega_i^2 \tag{8}$$

Since the two rotors rotate in opposite directon, the drag torques of the rotors can be expressed as:

$$M_{rotor} = \begin{bmatrix} 0 \\ 0 \\ k_{M,up}\omega_{up}^2 - k_{M,dw}\omega_{dw}^2 \end{bmatrix} \tag{9}$$

C. DUCT

In this paper, we use the simplified Bernoulli's principle to analyze the state of 0-1 and 2-3 in hover flight, which is shown in Fig. 3. The expression for the relationship between different states is given as:

$$\begin{cases} p_0 + \frac{1}{2}\rho v_0^2 = p_1 + \frac{1}{2}\rho v_i^2 \\ p_2 + \frac{1}{2}\rho v_i^2 = p_0 + \frac{1}{2}\rho v_e^2 \end{cases} \tag{10}$$

where p_0, p_1, p_2 represent the hydrostatic pressure of position 0, 1, and 2. $\boldsymbol{v_0}$ represents the velocity of the air outside the air cone formed by the rotation of rotors. $\boldsymbol{v_i}$ represents the rotor induced velocity. $\boldsymbol{v_e}$ represents the air velocity inside the air cone formed by the rotation of rotors.

Due to the Coanda effect, the airflow tends to follow the direction of the duct contour. As a result, the wake will have a larger area than that of a traditional helicopter. Comparing with a traditional helicopter, the wake of the duct has a larger area, which can provide additional thrust. As shown in [37], the equation to determine the thrust produced by both of the rotors and the duct is given by:

$$\begin{aligned} T &= \dot{m}v = \rho A v_i \left(v_e - v_0\right) \\ T &= T_{rotor} + T_{duct} \end{aligned} \tag{11}$$

with:

$$\begin{aligned} v_i &= a_d v_e \\ A_e &= a_d A \end{aligned} \tag{12}$$

where a_d represents the radio between the area of the wake and the disc formed by the propellers when they are rotating. The thrust experienced by the duct can be now expressed as:

$$\begin{aligned} \frac{T_{rotor}}{T} &= \frac{1}{2a_d} \\ T_{duct} &= \left(2a_d - 1\right) T_{rotor} \end{aligned} \tag{13}$$

The force on the vehicle generated by the duct is given as follows:

$$F_{duct} = \begin{bmatrix} 0 \\ 0 \\ \left(2a_d - 1\right)\left(k_{M,up}\omega_{up}^2 - k_{M,dw}\omega_{dw}^2\right) \end{bmatrix} \tag{14}$$

D. CONTROL VANES

The control surfaces consist of four sets of vanes with one set in each quadrant of the duct. The configuration of these vanes are shown in the Fig. 4. Vane 1 and vane 3 are deflected symmetrically to control the pitch angle. Similarly, vanes 2 are used for roll control. Vane 1 and vane 3 are deflected differently to realize yaw control.

The rudder control torque is

$$L = \frac{1}{2}\rho \upsilon_r^2 S_r C_{Lr}\left(\delta\right) \tag{15}$$

In which C_{Lr} is dimensionless lift coefficient, v_r is the air velocity through the vanes, S_r is the rudder surface area and δ represents the control vane deflection. Hence, the components of the lift forces and the moments created by the forces which are acting in the vehicle's body axes is given as

$$F_{vane} = \begin{bmatrix} \frac{1}{2}\rho v_r^2 S_{\mathrm{r}} C_{Lr}\left(\delta_1\right) + \frac{1}{2}\rho_r v_r^2 S_{\mathrm{r}} C_{Lr}\left(\delta_3\right) \\ \rho_r v_r^2 S_{\mathrm{r}} C_{Lr}\left(\delta_2\right) \\ 0 \end{bmatrix} \tag{16}$$

$$M_{vane} = \begin{bmatrix} \rho_r v_r^2 S_{\mathrm{r}} C_{Lr}\left(\delta_2\right) l_{2z} \\ \frac{1}{2}\rho v_r^2 S_{\mathrm{r}} C_{Lr}\left(\delta_1\right) l_{1z} + \frac{1}{2}\rho_r v_r^2 S_{\mathrm{r}} C_{Lr}\left(\delta_3\right) l_{3z} \\ \frac{1}{2}\rho v_r^2 S_{\mathrm{r}} C_{Lr}\left(\delta_1\right) l_{1x} - \frac{1}{2}\rho_r v_r^2 S_{\mathrm{r}} C_{Lr}\left(\delta_3\right) l_{3x} \end{bmatrix} \tag{17}$$

where $l_{1x}, l_{3x}, l_{1z}, l_{2z}, l_{3z}$ represent the x-components and z-components of the distances between the vehicle center

of gravity and the vane aerodynamic center. The effect of the drag forces and moments has been neglected for simplification.

E. GYROSCOPIC MOMENT

The spinning rotors of the ducted fan UAV will cause the gyroscopic precession torque effect. the expression for this moment vector is given as follows:

$$M_{gyro} = \begin{bmatrix} nI_{zprop}q\left(\omega_{up} - \omega_{down}\right) \\ -nI_{zprop}p\left(\omega_{up} - \omega_{down}\right) \\ 0 \end{bmatrix} \tag{18}$$

where I_{zprop} is the component of the rotors inertia about its spin axis.

The ducted coaxial-rotor UAV dynamics and kinematics equations are given as

$$\begin{cases} \dot{u} = vr - qw + \dfrac{1}{m}F_x \\ \dot{v} = pw - ur + \dfrac{1}{m}F_y \\ \dot{w} = uq - pv + \dfrac{1}{m}F_z \\ \dot{p} = -\dfrac{I_{zx}}{I_{xx}}(\dot{r} + pq) + \dfrac{I_{xy}}{I_{xx}}(pr - \dot{q}) + \dfrac{(I_{yy} - I_{zz})}{I_{xx}}qr \\ \qquad + \dfrac{I_{yz}}{I_{xx}}(r^2 - q^2) + \dfrac{1}{I_{xx}}M_x \\ \dot{q} = -\dfrac{I_{xx}}{I_{yy}}pr - \dfrac{I_{xy}}{I_{yy}}(\dot{p} + qr) + \dfrac{I_{yz}}{I_{yy}}(pq - \dot{r}) \\ \qquad + \dfrac{I_{xz}}{I_{yy}}(p^2 - qr) + \dfrac{I_{zz}}{I_{yy}}pq + \dfrac{1}{I_{yy}}M_y \\ \dot{r} = \dfrac{(I_{yy} - I_{xx})}{I_{zz}}pq + \dfrac{I_{xy}}{I_{zz}}(q^2 - p^2) - \dfrac{I_{yz}}{I_{zz}}(\dot{q} + pr) \\ \qquad + \dfrac{I_{xz}}{I_{zz}}(qr - \dot{p}) + \dfrac{1}{I_{zz}}M_z \\ \dot{\phi} = p + \tan\theta\,(q\sin\theta + r\cos\phi) \\ \dot{\theta} = q\cos\phi - r\sin\phi \\ \dot{\psi} = (q\sin\phi + r\cos\phi)\sec\theta \end{cases} \tag{19}$$

In hovering condition, we use small perturbation theory and the Taylor expansion to linearize the nonlinear model at the equilibrium point: $\dot{u} = \dot{v} = \dot{w} = 0, C\dot{p} = \dot{q} = \dot{r} = 0$. The nonlinear system can be linearized:

$$\begin{aligned} \dot{x}(t) &= A(t)x(t) + B(t)u(t) \\ y(t) &= C(t)x(t) + D(t)u(t) \end{aligned} \tag{20}$$

where the state vector $x = [p, q, r, \varphi, \theta, \psi]^T$, control input $u = [\delta_1, \delta_2, \delta_3]^T$ and output vector $y = [\varphi, \theta, \psi]^T$.

The nominal system matrixes A and B have been obtained by theoretical calculation, system identification and some flight tests in hovering condition. The process will not be detailed in this paper, the results are as follows:

$$A = \begin{bmatrix} 0 & 0.546 & 0 & 0 & 0 & 0 \\ -0.548 & 0 & 0 & 0 & 0 & 0 \\ 0 & 0 & 0 & 0 & 0 & 0 \\ 1 & 0 & 0 & 0 & 0 & 0 \\ 0 & 1 & 0 & 0 & 0 & 0 \\ 0 & 0 & 1 & 0 & 0 & 0 \end{bmatrix},$$

$$B = \begin{bmatrix} -0.1154 & 35.5267 & 0.1154 \\ -17.8150 & 0 & -17.8150 \\ -36.8704 & 0 & 36.8704 \\ 0 & 0 & 0 \\ 0 & 0 & 0 \\ 0 & 0 & 0 \end{bmatrix}$$

$$C = \begin{bmatrix} 1 & 0 & 0 & 0 & 0 & 0 \\ 0 & 1 & 0 & 0 & 0 & 0 \\ 0 & 0 & 1 & 0 & 0 & 0 \\ 0 & 0 & 0 & 1 & 0 & 0 \\ 0 & 0 & 0 & 0 & 1 & 0 \\ 0 & 0 & 0 & 0 & 0 & 1 \end{bmatrix} D = 0$$

III. PROBLEM FORMULATION AND PRELIMINARIES

A. PROBLEM FORMULATION

Considering the disturbances, model uncertainties and sensor fault, we introduce $d(t)$, ΔA and $f_s(t)$ in the ducted coaxial-rotor UAV model (20) setup in section II, which is described as

$$\begin{aligned} \dot{x}(t) &= (A + \Delta A)x(t) + Bu(t) + B_d d(t) \\ y(t) &= C_1 x(t) + f_s(t) \\ z(t) &= C_2 x(t) \end{aligned} \tag{21}$$

where $x(t) \in \Re^n$ is the system state vector, $u(t) \in \Re^r$ is the control input, $d(t) \in \Re^q$ is the unknown input vector and disturbance signal, $f_s(t) \in \Re^f$ is the sensor fault signal, $y(t) \in \Re^y$ and $z(t) \in \Re^z$ are the measurement output and performance output. A, B, B_d, C_1, C_2 and D_2 are kown matrices with appropriate dimensions, ΔA represents time-varying parameter uncertainties of system, defined in the following form: [44]

$$\Delta A = HF(t)G \tag{22}$$

$$F(t)^T F(t) \le I \tag{23}$$

where H and G are given matrices of appropriate dimensions, which can describe the structured uncertainties of the system precisely.

The observer-based controller is designed to detect faults and meet some desired control objectives. We use the state-feedback controller

$$u(t) = -K\hat{x}(t) \tag{24}$$

where K is the controller gain to be designed.

Then, we have the observer-based controller

$$\begin{aligned} \dot{\hat{x}}(t) &= (A + \Delta)\hat{x}(t) + Bu(t) + L\left(y(t) - \hat{y}(t)\right) \\ \hat{y}(t) &= C_1\hat{x}(t) \\ r(t) &= y(t) - \hat{y}(t) \\ u(t) &= -K\hat{x}(t) \end{aligned} \tag{25}$$

where L is the observer gain to be designed, $\hat{x}(t)$ is the estimate of $x(t)$, $r(t)$ is the generated residual.

Denoting $e(t) = x(t) - \hat{x}(t)$, $\hat{f}(t) = r(t) - f_s(t)$ $\tilde{x} = \left[x^T, e^T\right]^T$, where $e(t)$ is the state estimation error, $\hat{f}(t)$ is the sensor fault estimation error. Hence, we can write the augmented error system as

$$\dot{\tilde{x}}(t) = \bar{A}\tilde{x}(t) + \bar{B}_d d(t) + \bar{B}_{fs} f(t)$$

$$\hat{f}(t) = \bar{C}_1 \tilde{x}(t)$$
$$z(t) = \bar{C}_2 \tilde{x}(t) \tag{26}$$

Thus, the closed-loop state matrices are obtained as

$$\bar{A} = \begin{bmatrix} A + \Delta A - BK & BK \\ 0 & A + \Delta A - LC_1 \end{bmatrix}$$
$$\bar{B}_d = \begin{bmatrix} B_d \\ B_d \end{bmatrix}, \quad \bar{B}_{fs} = \begin{bmatrix} 0 \\ -L \end{bmatrix}$$
$$\bar{C}_1 = \begin{bmatrix} 0 & C_1 \end{bmatrix}, \quad \bar{C}_2 = \begin{bmatrix} C_2 & 0 \end{bmatrix} \tag{27}$$

The scheme of observer-based simultaneous flight control and sensor fault detection is shown in Fig. 5.

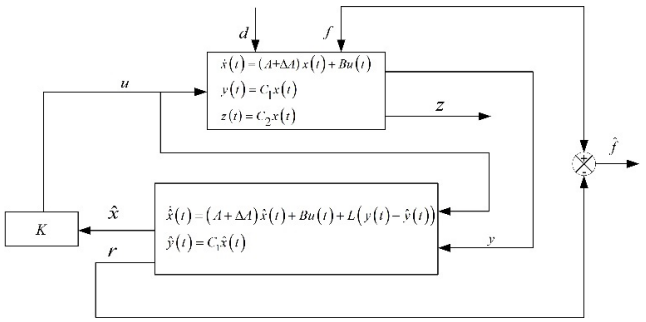

FIGURE 5. The scheme of simultaneous sensor fault detection and control.

Then, the simultaneous sensor fault detection and attitude control problem in hover condititon to be addressed in this paper can be expressed as follows.

Consider the new augmented system described by (26), we propose our design objectives as follows:

1) For control objective, we use the H_∞ norm constraint to guarantee robust stability of the closed-loop system. The constraint $\|G_{zd}(j\omega)\|_\infty < \gamma$ can minimise the effects of the disturbances on the performance output $z(t)$ in the presence of model uncertainties.

2) For detection objective, we ues the H_- to measure the fault sensitivity. The constraint is $\left\|G_{\hat{f}f_s}(j\omega)\right\|_- > \beta$ useful to increase the sensitivity of faults to the sensor fault estimation error.

3) For the stability of the closed-loop system, we use regional pole constrraints to place the ploes in the left-half plane, which can be defined as:

$$\{s \in \mathbb{C} : s + \bar{s} < 0\}$$

where

$$G_{zd}(j\omega) = \bar{C}_2 \left(j\omega I - \bar{A}\right)^{-1} \bar{B}_d$$
$$G_{\hat{f}f_s}(j\omega) = \bar{C}_1 \left(j\omega I - \bar{A}\right)^{-1} \bar{B}_{f_s}$$

B. PRELIMINARIES

The following lemmas are essential for the later developments

Lemma 1 [50]: (Finsler's Lemma): Let $\xi \in \mathbb{C}^n$, $L \in \mathbb{C}^{n\times n}$ and $H \in \mathbb{C}^{n\times m}$. Let $H^\perp$ be any matrix such that $H^\perp H = 0$. The following statements are equivalent:

(i) $\xi^* L \xi < 0, \quad \forall H^* \xi = 0, \ \xi \neq 0,$

(ii) $H^\perp L H^{\perp^T} < 0,$

(iii) $\exists \chi \in \Re^{m\times n} : L + H\chi + \chi^* H^* < 0,$

(iv) $\exists \mu \in \Re : L - \mu H H^T < 0.$

Lemma 2: Let Γ, W, and Λ be given matrices, there exists a matrix F satisfying

$$\Gamma F W + (\Gamma F W)^T + \Lambda < 0$$

If and only if the following two conditions hold

$$\Gamma^\perp \Lambda \Gamma^{\perp T} < 0$$
$$W^{T^\perp} \Lambda W^{T^{\perp T}} < 0$$

Lemma 3 [30]: (Generalised KYP lemma): Considering system $G(j\omega) = C(j\omega \text{I-A})^{-1} B + D$, let a sysmetric matrix Π with appropriate dimensions be given, the following statements are equivalent:

(i) The finite frequency inequality

$$\begin{bmatrix} G(j\omega) \\ I \end{bmatrix}^* \prod \begin{bmatrix} G(j\omega) \\ I \end{bmatrix} < 0, \quad \forall \omega \in \begin{bmatrix} -\omega_l & \omega_l \end{bmatrix}$$

(ii) There exists Hermitian matrices P and $Q > 0$ satisfying

$$\begin{bmatrix} A & I \\ C & 0 \end{bmatrix}^T \Xi \begin{bmatrix} A & I \\ C & 0 \end{bmatrix} + \begin{bmatrix} B & 0 \\ D & I \end{bmatrix}^T \Pi \begin{bmatrix} B & 0 \\ D & I \end{bmatrix} < 0$$

where

$$\Xi = \begin{bmatrix} -Q & P \\ P & \varpi_l^2 Q \end{bmatrix}$$

Lemma 4 [38] (H_∞ performance): Let $\|T(s)\|_\infty$ denote the H_∞ norm to $T(s)$, where $T(s) = C(\text{sI-A})^{-1} B + D$ is the continumous-time system. Then, the following three conditions are equivalent.

(i) Matrix A is stable and the H_∞ performance is bounded by $\gamma > 0$. Namely, $\|T(s)\|_\infty < \gamma$.

(ii) There exists a symmetric positive-definite matrix P to satisfy

$$\begin{bmatrix} AP + PA^T & PC^T & B \\ CP & -\gamma I & D \\ B^T & D^T & -\gamma I \end{bmatrix} < 0$$

(iii) There exists a symmetric positive-definite matrix P and a general matrix F satisfying

$$\begin{bmatrix} AF + F^T A^T & P - F^T + r_\infty AF & F^T C^T & B \\ P - F + r_\infty A^T F^T & -r_\infty \left(F + F^T\right) & r_\infty F^T C^T & 0 \\ CF & r_\infty CF & -\gamma I & D \\ B^T & 0 & D^T & -\gamma I \end{bmatrix} < 0$$

For a sufficiently small scalar $r_\infty > 0$.

Lemma 5 [39]: Let X, Y and F be real matrices of appropriate dimension with $F^T F \leq I$, then, for any scalar $\varepsilon > 0$,

$$X^T F Y + Y^T F^T X^T \leq \varepsilon^{-1} X^T X + \varepsilon Y^T Y$$

Lemma 6 [40]: Let $S = \begin{bmatrix} S_{11} & S_{12} \\ S_{12}^T & S_{22} \end{bmatrix}$ be symmetric matrix of S_{11}, S_{12}, S_{22} with appropriate dimensions satisfying $S_{11} = S_{11}^T$, $S_{12} = S_{12}^T$. then the following propositions are equivalent:

(i) $S < 0$
(ii) $S_{11} < 0, \quad S_{22} - S_{12}^T S_{11}^{-1} S_{12} < 0$
(iii) $S_{22} < 0, \quad S_{11} - S_{12} S_{22}^{-1} S_{12}^T < 0$

IV. SIMULTANEOUS FAULT DETECTION AND CONTROL

A robust control and fault detection approach based on observer technique is proposed to solve the hovering attitude control problem for a ducted coaxial-rotor UAV in the presence of unknown disturbance, system uncertainties and sensor fault. The aim of the proposed methodology is to give a design technique that guarantees the robustness to disturbances and uncertainties and sensitivity of faults of the UAV. In addition, the stability problem of the UAV can be satisfied by the Lyapunov theorem.

In this section, the LMI formulation for solving the simultaneous fault detection and control problem would be given. The main results are summarized in Theorems 1-7, such that a desired integrated detector/controller could be constructed.

A. CONDITIONS FOR CONTROL PERFORMANCE

Recall lemma 4, we can get the following inequality which can guarantee the prescribed H_∞ performance level $\gamma > 0$ of the closed-loop system (26)

$$\begin{bmatrix} \bar{A}F + F^T\bar{A}^T & P - F^T + r_\infty \bar{A}F & F^T\bar{C}_2^T & \bar{B}_d \\ P - F + r_\infty \bar{A}^T F^T & -r_\infty\left(F + F^T\right) & r_\infty F^T \bar{C}_2^T & 0 \\ \bar{C}_2 F & r_\infty \bar{C}_2 F & -\gamma I & D \\ \bar{B}_d^T & 0 & D^T & -\gamma I \end{bmatrix} < 0 \tag{28}$$

Notice that, the augmented matrix $\bar{A}$ is complicated and contains the system time-vary uncertainties, controller gain and observer gain to be designed, in order to linearize the design conditions and make the inequality solvable, we need to introduce the following change of variables [42]. Clearly, this critical and special structure of the variables is stringent and brings conservatism into the proposed method design.

We introduce the following change of variables F and F^{-1} as

$$\begin{aligned} F &= \begin{bmatrix} X & \left(I - XY^T\right)V^{-T} \\ U & -UY^T V^{-T} \end{bmatrix} \\ F^{-1} &= \begin{bmatrix} Y^T & \left(I - Y^T X\right)U^{-1} \\ V^T & -V^T X U^{-1} \end{bmatrix} \end{aligned} \tag{29}$$

where matrices X, Y are symmetric and U, V and X are invertible.

In addition, a transformation matrix has been introduced

$$T = \begin{bmatrix} I & 0 \\ Y & V \end{bmatrix} \tag{30}$$

Define

$$\begin{aligned} \hat{A} &= T\bar{A}FT^T \\ &= \begin{bmatrix} (A + \Delta A)X - NX + NU & A + \Delta A - N \\ M & YA - YN \end{bmatrix} \\ \hat{B}_d &= T\bar{B}_d = \begin{bmatrix} B_d \\ YB_d + VB_d \end{bmatrix} \end{aligned} \tag{31}$$

$$\begin{aligned} \hat{B}_{f_s} &= T\bar{B}_{f_s} = \begin{bmatrix} 0 \\ -VL \end{bmatrix} \\ \hat{C}_1 &= \bar{C}_1 F T^T = \begin{bmatrix} C_1 U & 0 \end{bmatrix} \\ \hat{C}_2 &= \bar{C}_2 F T^T = \begin{bmatrix} C_2 X & C_2 \end{bmatrix} \\ \hat{F} &= TFT^T = \begin{bmatrix} X & I \\ Z & Y \end{bmatrix} \end{aligned} \tag{32}$$

where $Z = XY + VU$.

Then the control objective 1) is transformed to an inequality condition in the following theorem:

Theorem 1: Consider the augmented system (26), given positive scalar γ, the H_∞ performance $\|G_{zd}(j\omega)\|_\infty < \gamma$ holds if, for some positive scalar r_∞, there exists a solution $\left(X, Y, M, N, Z, \hat{P}\right)$ to the following LMI

$$\begin{bmatrix} \hat{A} + \hat{A}^T & \hat{P} - \hat{F}^T + r_\infty \hat{A} & \hat{C}_2^T & \hat{B}_d \\ * & -r_\infty\left(\hat{F} + \hat{F}^T\right) & r_\infty \hat{C}_2^T & 0 \\ * & * & -\gamma I & 0 \\ * & * & * & -\gamma I \end{bmatrix} < 0 \tag{33}$$

where $\hat{P}$ is a positive-definite matrix, and,

$$\begin{aligned} &\begin{bmatrix} \hat{A} & \hat{B}_d \\ \hat{C}_2 & 0 \end{bmatrix} \\ &= \begin{bmatrix} (A + \Delta A)X + BG & A + \Delta A - BH & B_d \\ M + Y\Delta AX + V\Delta AU & Y(A + \Delta A) - N & YB_d + VB_d \\ C_2 X & C_2 & 0 \end{bmatrix} \end{aligned} \tag{34}$$

where the change of observer and controller variables are defined as follows

$$\begin{aligned} &\begin{bmatrix} M & N \\ G & H \end{bmatrix} \\ &= \begin{bmatrix} YAX + VAU & 0 \\ 0 & 0 \end{bmatrix} + \begin{bmatrix} YB & -V \\ I & 0 \end{bmatrix} \begin{bmatrix} K & 0 \\ 0 & L \end{bmatrix} \begin{bmatrix} U - X & I \\ C_1 U & 0 \end{bmatrix} \end{aligned} \tag{35}$$

Proof: By premultiplying and postmultiplying diag $\{T, T, I, I\}$ and diag $\left\{T^T, T^T, I, I\right\}$ on inequality (28), we can get the Theorem 1. It is worth noting that the nonlinear terms in the simultaneous fault detection and control augmented system of our UAV makes it impossible to directly apply Lemma 4. The problem is solved by the changes of variables, then the H_∞ performance of the designed system can be guaranteed.

However, there are uncertainty terms ΔA in inequality (33). In practical engineering, the uncertain parameters are unknown, so we need a condition for the existence of the controller and the observer which are independent of the uncertain parameters. That is the following theorem:

Theorem 2: For the augmented system (26) with uncertainties and performance $\|G_{zd}(j\omega)\|_\infty < \gamma$, given positive scalar γ, positive real number ε_1 and some positive scalar r_∞, if there exists a solution $\left(X, Y, M, N, Z, \hat{P}\right)$, and $\hat{P}$ is

a positive-definite matrix, the following LMI

$$\begin{bmatrix} \hat{A}_1+\hat{A}_1^T & \hat{P}-\hat{F}^T+r_\infty\hat{A}_1 & \hat{C}_2^T & \hat{B}_d & G_1^T & \varepsilon_1 \mathrm{H}_1^T \\ * & -r_\infty\left(\hat{F}+\hat{F}^T\right) & r_\infty\hat{C}_2^T & 0 & 0 & 0 \\ * & * & -\gamma I & 0 & 0 & 0 \\ * & * & * & -\gamma I & 0 & 0 \\ * & * & * & * & -\varepsilon_1 I & 0 \\ * & * & * & * & * & -\varepsilon_1 I \end{bmatrix} < 0 \tag{36}$$

holds, then the designed controller gain K and the observer gain L can guarantee the H_∞ robust performance of the system (26).

Proof: The inequality (33) is equivalent to

$$\Omega_1 + \Delta\Omega_1 < 0$$

where

$$\Omega_1 = \begin{bmatrix} \hat{A}_1+\hat{A}_1^T & \hat{P}-\hat{F}^T+r_\infty\hat{A}_1 & \hat{C}_2^T & \hat{B}_d \\ * & -r_\infty\left(\hat{F}+\hat{F}^T\right) & r_\infty\hat{C}_2^T & 0 \\ * & * & -\gamma I & 0 \\ * & * & * & -\gamma I \end{bmatrix}$$

$$\Delta\Omega_1 = \begin{bmatrix} \Delta\hat{A}+\Delta\hat{A}^T & r_\infty\Delta\hat{A} & 0 & 0 \\ * & 0 & 0 & 0 \\ 0 & 0 & 0 & 0 \\ 0 & 0 & 0 & 0 \end{bmatrix}$$

$$\begin{aligned} \hat{A} &= \hat{A}_1 + \Delta\hat{A} \\ &= \begin{bmatrix} AX+BG & A-BH \\ M & YA-N \end{bmatrix} + \begin{bmatrix} \Delta AX & \Delta A \\ Y\Delta AX+V\Delta AU & Y\Delta A \end{bmatrix} \end{aligned}$$

Since $\Delta A = HF(t)G$, we can get

$$\Omega_1 + \begin{bmatrix} \Delta_{11} & \Delta_{12} & \Delta_{13} & \Delta_{14} & 0 & 0 \\ \Delta_{12}^T & \Delta_{22} & \Delta_{23} & \Delta_{24} & 0 & 0 \\ \Delta_{13}^T & \Delta_{23}^T & 0 & 0 & 0 & 0 \\ \Delta_{14}^T & \Delta_{24}^T & 0 & 0 & 0 & 0 \\ 0 & 0 & 0 & 0 & 0 & 0 \\ 0 & 0 & 0 & 0 & 0 & 0 \end{bmatrix} < 0$$

where

$$\begin{aligned} \Delta_{11} &= (HFG)X + X^T(HFG)^T \\ \Delta_{12} &= (HFG) + X^T(HFG)^T Y^T + U^T(HFG)^T V^T \\ \Delta_{22} &= Y(HFG) + (HFG)^T Y^T \\ \Delta_{13} &= r_\infty(HFG)X \\ \Delta_{14} &= r_\infty(HFG) \\ \Delta_{23} &= r_\infty Y(HFG)X + r_\infty V(HFG)U \\ \Delta_{24} &= r_\infty Y(HFG) \end{aligned}$$

$$\begin{aligned} &\Delta\Omega_1 \\ &= \begin{bmatrix} H & 0 & 0 & 0 \\ YH & VH & 0 & 0 \\ 0 & 0 & 0 & 0 \\ 0 & 0 & 0 & 0 \end{bmatrix} F \begin{bmatrix} GX & G & r_\infty GX & r_\infty G \\ GU & 0 & r_\infty GU & I \\ 0 & 0 & 0 & 0 \\ 0 & 0 & 0 & 0 \end{bmatrix} \\ &+ \begin{bmatrix} GX & G & r_\infty GX & r_\infty G \\ GU & 0 & r_\infty GU & I \\ 0 & 0 & 0 & 0 \\ 0 & 0 & 0 & 0 \end{bmatrix}^T F^T \begin{bmatrix} H & 0 & 0 & 0 \\ YH & VH & 0 & 0 \\ 0 & 0 & 0 & 0 \\ 0 & 0 & 0 & 0 \end{bmatrix}^T \end{aligned}$$

By lemma 5, for any scalar $\varepsilon_1 > 0$, we can get

$$\Omega_1 + \varepsilon_1 \mathrm{H}_1\mathrm{H}_1^T + \varepsilon_1^{-1} G_1 G_1^T < 0 \tag{37}$$

where

$$\mathrm{H}_1 = \begin{bmatrix} H & 0 & 0 & 0 \\ YH & VH & 0 & 0 \\ 0 & 0 & 0 & 0 \\ 0 & 0 & 0 & 0 \end{bmatrix}, G_1 = \begin{bmatrix} GX & G & r_\infty GX & r_\infty G \\ GU & 0 & r_\infty GU & I \\ 0 & 0 & 0 & 0 \\ 0 & 0 & 0 & 0 \end{bmatrix}$$

Then, by lemma 6, the inequality (37) is equivalent to

$$\begin{bmatrix} \Omega_1 & G_1^T & \mathrm{H}_1 \\ G_1 & -\varepsilon_1 I & 0 \\ \mathrm{H}_1^T & 0 & \varepsilon_1^{-1} I \end{bmatrix} < 0 \tag{38}$$

By premultiplyilng and postmultiplying diag $\{I, I, \varepsilon I\}$ on the inequality (38), we can get the Theorem 2, which completes the proof.

Hence, Theorem 1 can be solved in the existence of the time-varying and unknown uncertainties. Based on Theorem 1, we can get Theorem 2, the sufficient condition of existence for augmented error system (26) without model parameter uncertainty ΔA is given.

B. CONDITIONS FOR FAULT DETECTION SENSITIVITY

Consider system (26), the sensor faults considered in this paper are assumed to be in the low frequency domain, by lemma 3, the following statements are equivalent:

(i) $\|G_{\hat{f}f_s}(j\omega)\|_- > \beta$

(ii)

$$\begin{bmatrix} \bar{A} & I \\ \bar{C}_1 & 0 \end{bmatrix} \Phi \begin{bmatrix} \bar{A} & I \\ \bar{C}_1 & 0 \end{bmatrix}^T + \begin{bmatrix} \bar{B}_f & 0 \\ 0 & I \end{bmatrix} \Pi \begin{bmatrix} \bar{B}_f & 0 \\ 0 & I \end{bmatrix}^T < 0 \tag{39}$$

where $\Phi = \begin{bmatrix} -Q & P_1 \\ P_1 & \varpi_l^2 Q \end{bmatrix}$, $\Pi = \begin{bmatrix} -I & 0 \\ 0 & \beta^2 I \end{bmatrix}$, P_1 is a symmetric matrix and Q is a positive-definite matrix.

Since we focus on augmented error system with low frequency sensor fault, disturbances and model parameter uncertainty, we need to design an new approach to accurately characterise the low-frequency performance index and the existence of this method does not depend on the information of system uncertainties. Different from most existing techniques, better fault sensitivity can be achieved by accurately characterizing the finite frequency performance index.

The detection objective 2) is transformed to an inequality condition in the following theorem:

Theorem 3: Given augmented system (26), the low frequency domain sensor fault sensitivity condition $\left\|G_{\hat{f}f_s}(j\omega)\right\|_- > \beta$, for some positive scalar $\beta > 0$, holds if there exists a solution $\left(X, Y, M, N, Z, \hat{P}_1\right)$ to the following

LMI

$$\begin{bmatrix} -\hat{Q} & \hat{P}_1-\hat{F} & 0 & -\hat{F}\xi \\ * & \varpi_l^2\hat{Q}+He\left(\hat{A}+\xi\hat{B}_{fs}^T\right) & \hat{B}_{fs}-\xi I & \hat{A}\xi+\hat{C}_1^T \\ * & * & -2I & 0 \\ * & * & * & \beta^2 I+He\left(\hat{C}_1\xi\right) \end{bmatrix} < 0 \tag{40}$$

where $\hat{P}_1$, $\hat{Q}$ are symmetric matrices and $\hat{Q} > 0$.

Proof: Denoting

$$\Delta = \begin{bmatrix} \Phi & 0 \\ 0 & \begin{bmatrix} \bar{B}_f & 0 \\ 0 & I \end{bmatrix} \Pi \begin{bmatrix} \bar{B}_f & 0 \\ 0 & I \end{bmatrix}^T \end{bmatrix}$$

then, the inequality (38) can be reformulated as

$$\begin{bmatrix} \bar{A}^T & \bar{C}_1^T \\ I & 0 \\ 0 & I \end{bmatrix}^T \left(\begin{bmatrix} I & 0 & 0 \\ 0 & I & 0 \\ 0 & I & 0 \\ 0 & 0 & I \end{bmatrix}^T \Delta \begin{bmatrix} I & 0 & 0 \\ 0 & I & 0 \\ 0 & I & 0 \\ 0 & 0 & I \end{bmatrix} \right) \begin{bmatrix} \bar{A}^T & \bar{C}_1^T \\ I & 0 \\ 0 & I \end{bmatrix} < 0 \tag{41}$$

On the other hand,

$$\begin{bmatrix} I \\ 0 \\ 0 \end{bmatrix}^T \left(\begin{bmatrix} I & 0 & 0 \\ 0 & I & 0 \\ 0 & I & 0 \\ 0 & 0 & I \end{bmatrix}^T \Delta \begin{bmatrix} I & 0 & 0 \\ 0 & I & 0 \\ 0 & I & 0 \\ 0 & 0 & I \end{bmatrix} \right) \begin{bmatrix} I \\ 0 \\ 0 \end{bmatrix} = -Q < 0 \tag{42}$$

then by lemma 2, we have that (38) holds if and only if

$$\Theta + \begin{bmatrix} -I \\ \bar{A} \\ \bar{C}_1 \end{bmatrix} F_1 \begin{bmatrix} 0 & I & 0 \\ 0 & 0 & I \end{bmatrix} + \begin{bmatrix} 0 & I & 0 \\ 0 & 0 & I \end{bmatrix}^T F_1^T \begin{bmatrix} -I \\ \bar{A} \\ \bar{C}_1 \end{bmatrix}^T < 0 \tag{43}$$

where

$$\Theta = \begin{bmatrix} I & 0 & 0 \\ 0 & I & 0 \\ 0 & I & 0 \\ 0 & 0 & I \end{bmatrix}^T \Delta \begin{bmatrix} I & 0 & 0 \\ 0 & I & 0 \\ 0 & I & 0 \\ 0 & 0 & I \end{bmatrix} = \begin{bmatrix} -Q & P_1 & 0 \\ P_1 & \varpi_l^2 Q - \bar{B}_f \bar{B}_f^T & 0 \\ 0 & 0 & \beta^2 I \end{bmatrix}$$

In order to make the inequality being feasible, we need to partition F_1 as $F_1 = \begin{bmatrix} F_{11} & F_{12} \end{bmatrix}$, where $F_{11} = F, F_{12} = F\xi$, where ξ are given matrix, which guarantees that F_{12} has appropriate dimensions.

By premultiplying diag $\{T, T, I\}$ and postmultiplying diag $\left\{T^T, T^T, I\right\}$, we have

$$\begin{bmatrix} -\hat{Q} & \hat{P}_1 & 0 \\ * & \varpi_l^2\hat{Q} - \hat{B}_{f_s}\hat{B}_{f_s}^T & 0 \\ * & * & \beta^2 I \end{bmatrix} + He\left(\begin{bmatrix} -\hat{F} \\ \hat{A} \\ \hat{C}_1 \end{bmatrix} \begin{bmatrix} 0 & I & \xi \end{bmatrix} \right) < 0 \tag{44}$$

where $\hat{Q} = TQT^T$ and $\hat{P}_1 = TP_1T^T$, define

$$\Psi = \begin{bmatrix} I & 0 & 0 \\ 0 & I & 0 \\ 0 & \hat{B}_{fs}^T & 0 \\ 0 & 0 & I \end{bmatrix}$$

$$\Delta = \begin{bmatrix} -\hat{Q} & \hat{P}_1 - \hat{F} & 0 & -\hat{F}\xi \\ * & \varpi_l^2\hat{Q} + He\left(\hat{A}\right) & -I & \hat{A}\xi + \hat{C}_1^T \\ * & * & 0 & 0 \\ * & * & * & \beta^2 I + He\left(\hat{C}_1\xi\right) \end{bmatrix} \tag{45}$$

Then, (44) is rewritten as

$$\Psi^T \Delta \Psi < 0 \tag{46}$$

Recall lemma 1, we have that (46) holds if and only if there exists matrix Λ that

$$\Delta + \Lambda\Phi + \Phi^T\Lambda^T < 0$$

where

$$\Phi^{T^\perp} = \begin{bmatrix} 0 \\ \hat{B}_{fs} \\ -I \\ 0 \end{bmatrix}^\perp = \begin{bmatrix} I & 0 & 0 \\ 0 & I & 0 \\ 0 & \hat{B}_{fs}^T & 0 \\ 0 & 0 & I \end{bmatrix}, \quad \Lambda^T = \begin{bmatrix} 0 \\ \xi \\ I \\ 0 \end{bmatrix}$$

finally, after calculation, we get the theorem 3, which completes the proof.

Notice that there are also uncertainty terms ΔA in inequality (40), by following the similar proof procedure of theorem 2, we can obtain the sufficient codition of existence for augmented error system (26) without model parameter uncertainty ΔA is given. The proof is omitted for the sake of brevity.

The LMI constraints for the low-frequency sensor fault detection sensitivity is given in the following theorem:

Theorem 4: For the augmented system (26) with uncertainties and performance $\left\| G_{\hat{f}f_s}(j\omega) \right\|_- > \beta$, given positive scalar β and positive real number ε_2 , if there exists a solution $\left(X, Y, M, N, Z, \hat{P}_1\right)$, where $\hat{P}_1$, $\hat{Q}$, are symmetric matrices and $\hat{Q} > 0$, the LMI, (47), as shown at the bottom of the next page, holds, where

$$\mathrm{H}_2 = \begin{bmatrix} 0 & 0 & 0 & 0 & 0 & 0 \\ 0 & H & 0 & 0 & 0 & 0 \\ 0 & YH & VH & 0 & 0 & 0 \\ 0 & 0 & 0 & 0 & 0 & 0 \\ 0 & 0 & 0 & 0 & 0 & 0 \\ 0 & 0 & 0 & 0 & 0 & 0 \end{bmatrix} \quad G_2 = \begin{bmatrix} 0 & 0 & 0 & 0 & 0 & 0 \\ 0 & GX & G & 0 & GX\xi & G\xi \\ 0 & GU & 0 & 0 & GU\xi & 0 \\ 0 & 0 & 0 & 0 & 0 & 0 \\ 0 & 0 & 0 & 0 & 0 & 0 \\ 0 & 0 & 0 & 0 & 0 & 0 \end{bmatrix}$$

then the designed controller gain K and the observer gain L can guarantee the low-frequency fault detection sensitivity performance of the system (26).

C. CONDITIONS FOR STABILITY

In order to achieve design objective 3), which is to guarantee the stability of the system and the dynamic performance of the closed-loop system, theorem 5 is proposed:

Theorem 5: Given augmented system (26), conditions for the stability of the closed-loop system holds if there exists a solution (X, Y, M, N, Z, P_2) to the following LMI

$$\begin{bmatrix} -rHe\left(\hat{F}_2\right) & \hat{P}_2 - q\hat{F}_2 + r\hat{A}^T \\ \hat{P}_2 - q\hat{F}_2^T + r\hat{A} & He\left(\hat{A}\right) \end{bmatrix} < 0 \tag{48}$$

with r, q are given positive scalars.

Proof: Consider the standard Lyapunov theorem, the matrix $\bar{A}$ has all its eigenvalues in the open left-half plane if and only if there exists a positive symmetric P_2 that the following inequality holds

$$\begin{bmatrix} \bar{A} & I \end{bmatrix} \begin{bmatrix} 0 & P_2 \\ P_2 & 0 \end{bmatrix} \begin{bmatrix} \bar{A} & I \end{bmatrix}^T = \bar{A}P_2 + P_2\bar{A} < 0 \quad (49)$$

On the other hand,

$$\begin{bmatrix} qI & -rI \end{bmatrix} \begin{bmatrix} 0 & P_2 \\ P_2 & 0 \end{bmatrix} \begin{bmatrix} qI & -rI \end{bmatrix}^T = -rqP - qrP < 0 \quad (50)$$

Explicit null space bases calculations yield

$$\begin{bmatrix} \bar{A} & I \end{bmatrix} = \begin{bmatrix} -I \\ \bar{A} \end{bmatrix}^{\perp}, \quad \begin{bmatrix} qI & -rI \end{bmatrix} = \begin{bmatrix} rI \\ qI \end{bmatrix}^{\perp}$$

Recall lemma 2, (49) and (50) hold that the following inequality holds if and only if there exists a matrix F_2 satisfying

$$\begin{bmatrix} 0 & P_2 \\ P_2 & 0 \end{bmatrix} + \begin{bmatrix} -I \\ \bar{A} \end{bmatrix} F_2 \begin{bmatrix} rI & qI \end{bmatrix} + \left(\begin{bmatrix} -I \\ \bar{A} \end{bmatrix} F_2 \begin{bmatrix} rI & qI \end{bmatrix} \right)^T < 0 \quad (51)$$

By premultiplying diag $\{T, T\}$ and postmultiplying diag $\left\{T^T, T^T\right\}$, we have the inequality (48), which complets the proof.

Obviously, the model parameter uncertainty term ΔA stiil makes it is impossible to solve the stability condition by theorem 5. Following the similar procedure of Theorem 2 and Theorem 4, we can obtain the stability sufficient condition for the system (26) without model parameter uncertainty ΔA is given.

Theorem 6: For the augmented system (26) with uncertainties and stability constraints of the closed-loop system, given positive scalar ε_3, if there exists a solution $\left(X, Y, M, N, Z, \hat{P}_2\right)$, where r, q are given positive scalars, and $\hat{P}_2$ is symmetric positive matrix, the following LMI

$$\begin{bmatrix} -rHe\left(\hat{F}_2\right) & \hat{P}_2 - q\hat{F}_2 + rA_1^T & G_3^T & \varepsilon_3 \mathrm{H}_3 \\ * & He\left(\hat{A}_1\right) & 0 & 0 \\ * & * & -\varepsilon_3 I & 0 \\ * & * & * & -\varepsilon_3 I \end{bmatrix} < 0 \quad (52)$$

holds, where

$$\mathrm{H}_3 = \begin{bmatrix} 0 & 0 & 0 & 0 \\ 0 & 0 & 0 & 0 \\ H & 0 & 0 & 0 \\ YH & VH & 0 & 0 \end{bmatrix},$$

TABLE 1. The parameters of the ducted coaxial-rotor UAV for simulations.

Symbol	Value	Unit
g	9.8	m/s²
m	6.56	kg
L	0.208	m
L'	0.129	m
$\mathrm{I_{xx}}$	0.345	kg·m²
$\mathrm{I_{yy}}$	0.345	kg·m²
$\mathrm{I_{zz}}$	0.081	kg·m²
$\mathrm{I_{zprop}}$	0.006	kg·m²
ρ_∞	1.22	kg/m³
$\mathrm{S_r}$	0.0138	m²
$\mathrm{v_i}$	20	m/s
$\mathrm{C_{Lr}}$	0.12	1
$\mathrm{C_{Dr}}$	0.12	1

$$G_3 = \begin{bmatrix} rGX & rG & GX & G \\ rGU & 0 & GU & 0 \\ 0 & 0 & 0 & 0 \\ 0 & 0 & 0 & 0 \end{bmatrix}$$

then the designed controller gain K and the observer gain L can guarantee the stability performance of the system (26).

D. ALGORITHM

According Theorems 1-6, simultaneous robust control and sensor fault detection problem considering system parameter uncertainty can be solved by the following theorem

Theorem 7: Cosider system (26), for given positive scalars $r_\infty, r, q, \gamma, \beta, \varepsilon_1, \varepsilon_2, \varepsilon_3$, there exist a observer-based controller (25) such that the augmented system (26) satisfying H_∞ performance $\|G_{zd}(j\omega)\|_\infty < \gamma$, low frequency domain sensor fault sensitivity condition $\left\|G_{\hat{f}f_s}(j\omega)\right\|_- > \beta$ and stability of the closed-loop system if the inequality conditions (35), (47), and (52) hold.

V. SIMULATIONS

In this section, the proposed control and detection strategy has been tested by simulation in order to illustrate the effectiveness and the performance attained for the ducted coaxial-rotor UAV control and sensor fault detection problem. The ducted coaxial-rotor UAV model parameters used in the simulations are displayed in Table 1.

Next, given $r_\infty = r = q = 1, \gamma = 0.6, \beta = 0.5$, $\varepsilon_1 = \varepsilon_2 = \varepsilon_3 = 1$, applying Theorem 7, we use the LMI toolbox and Simulation environment in the Matlab to

$$\begin{bmatrix} -\hat{Q} & \hat{P}_1 - \hat{F} & 0 & -\hat{F}\xi & G_2^T & \varepsilon_2 \mathrm{H}_2 \\ * & \varpi_l^2 \hat{Q} + He\left(\hat{A}_1 + \xi \hat{B}_{fs}^T\right) & \hat{B}_{fs} - \xi I & \hat{A}_1\xi + \hat{C}_1^T & 0 & 0 \\ * & * & -2I & 0 & 0 & 0 \\ * & * & * & \beta^2 I + He\left(\hat{C}_1\xi\right) & 0 & 0 \\ * & * & * & * & -\varepsilon_2 I & 0 \\ & * & * & * & * & -\varepsilon_2 I \end{bmatrix} < 0 \quad (47)$$

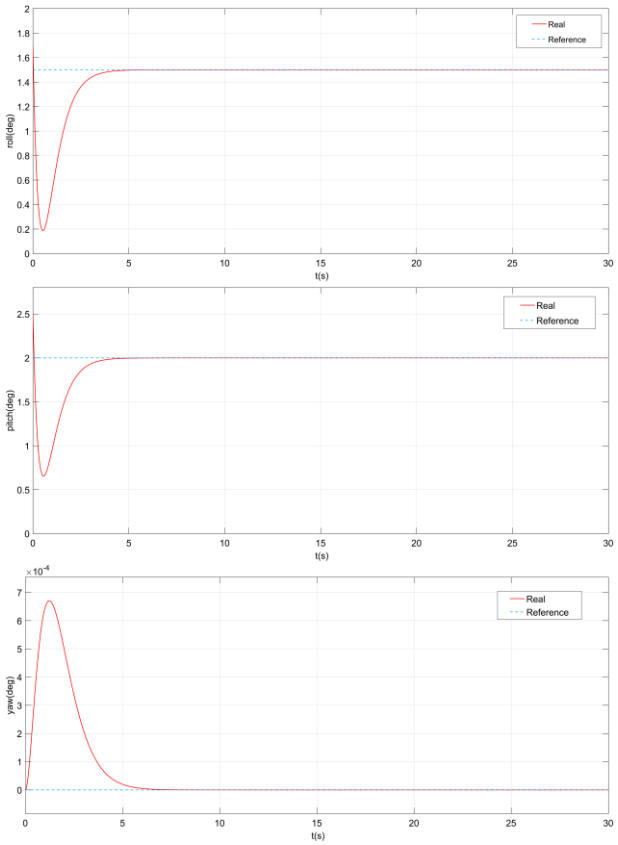

FIGURE 6. Attitude trajectories.

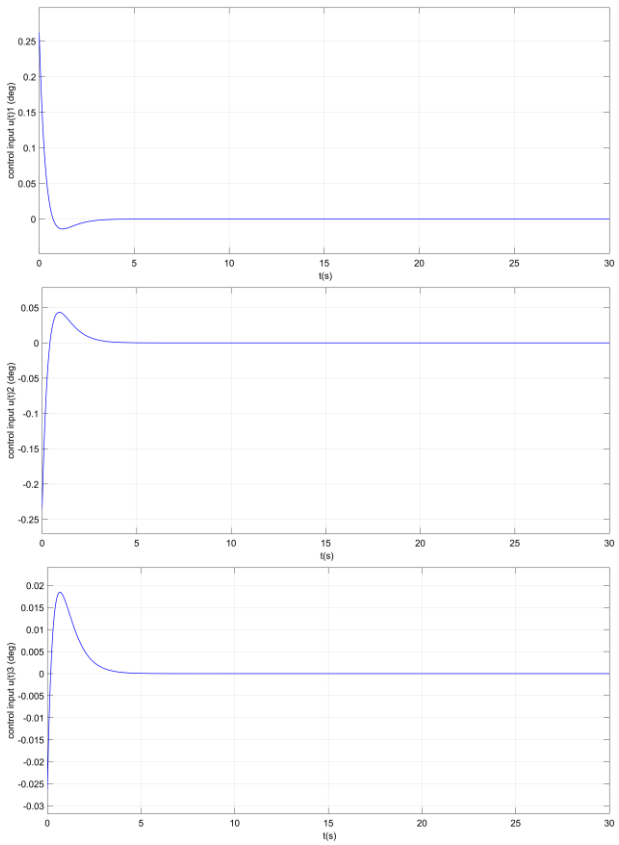

FIGURE 7. Control input signals.

illustrate the effectiveness of the proposed method, we get K and L, as shown at the bottom of this page.

A. FLIGHT WITHOUT DISTURBANCES AND FAULTS

To illustrate the attitude tracking control performance without disturbances, uncertainties and faults, the system intinal condition is set as $x(0) = \left[1.7\ 2.5\ 0\ 0\ 0\ 0\right]^{\mathrm{T}}$, $\hat{x}(0) = \left[0\ 0\ 0\ 0\ 0\ 0\right]^{T}$. The attitude tracking control performance and control input responses are shown in Fig. 6 and Fig. 7, respectively. All the attitude variables can track the reference command within 5s and the yaw channel is less affected by the other two channels. The system can converge quickly due to the proposed method. Finally, Fig. 7 illustrates that the control input signals all acceptable and could be applied to real model.

B. FLIGHT WITH DISTURBANCES, UNCERTAINTIES AND FAULTS

This part simulation is implemented to illustrate the control performance of the proposed method with taking into consideration the system parameter uncertainty, disturbance and constant deviation fault. The system initial condition is $x(0) = \left[0\ 0\ 0\ 0\ 0\ 0\right]^{T}$ and the observer initial condition is also $\hat{x}(0) = \left[0\ 0\ 0\ 0\ 0\ 0\right]^{T}$. Assume that $B_d = \left[0.71\ -0.53\ 0.80\ 1\ 1\ 1\right]^{T}$. The uncertainty of ΔA is assumed to be in the range [-40%, 40%], and the disturbance

$$K = \begin{bmatrix} -0.0154 & 0.1155 & -0.0555 & 0 & 0.1126 & -0.0544 \\ -0.1158 & -0.0154 & -0.0275 & -0.1129 & 0 & -0.0215 \\ -0.0153 & -0.1154 & 0.0561 & 0.0007 & 0.1120 & 0.0554 \end{bmatrix}$$

$$L = \begin{bmatrix} -1.1720 & -1.9563 & 0.0039 & 1.2190 & 0.2542 & 0.0369 \\ 0.8093 & -8.3594 & -0.0560 & -1.5583 & 0.7164 & -0.0255 \\ -0.0074 & 0.0179 & -0.1368 & -0.0095 & 0.0327 & -0.2888 \\ 0.8986 & 0.5610 & 0.0397 & -0.2324 & 2.8107 & 0.0842 \\ -2.2698 & 1.0911 & -0.0808 & -2.5524 & -0.1394 & -0.0959 \\ -0.0568 & 0.0608 & 1.3111 & -0.0904 & 0.0937 & -0.0357 \end{bmatrix}$$

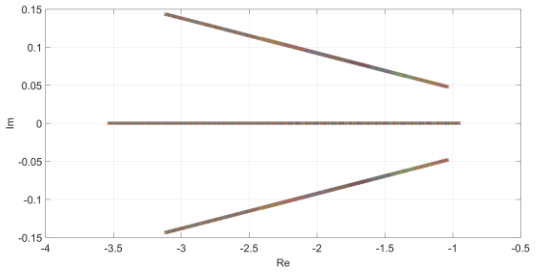

FIGURE 8. Closed loop poles with $\Delta \in [-40\%, 40\%]$.

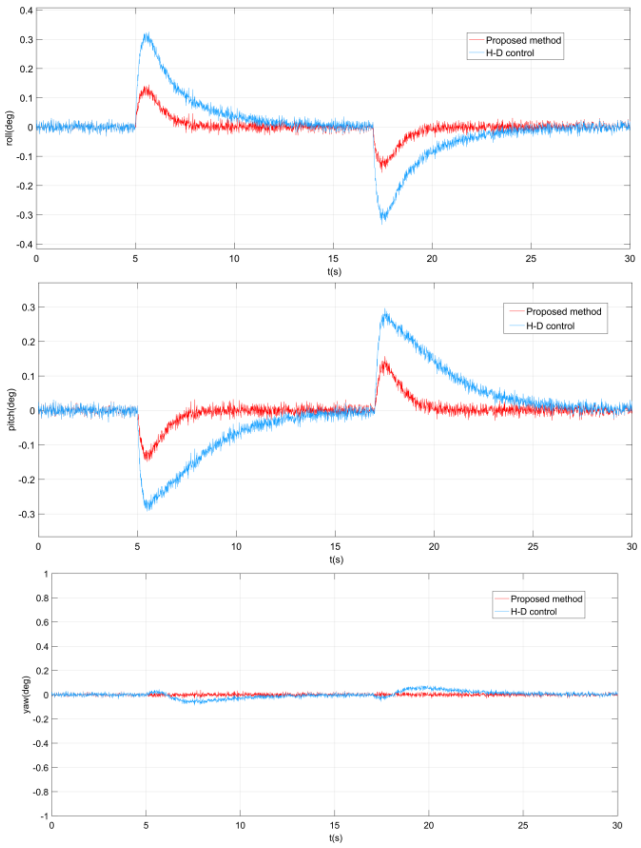

FIGURE 9. Altitude response performance using H-D control and proposed method.

$d(t)$ is assumed to be the random noise with power 0.0005. The low-frequency sensor fault $f_s(t)$ is considered as the X-axis and Y-axis angular velocity sensor constant gain fault, which is assumed to be $f_s(t) = 1$ for $5s \leq t \leq 17s$, and $f_s(t) = 0$ elsewhere. It is expected that in the presence of system uncertainty, disturbance and fault, the closed-loop system is still stable and robust to disturbance. It can be seen from Fig. 8 that the poles of the closed-loop system can be all placed in the left-half plan with the system parameter uncertainty vary in the range [-40%, 40%], which means the proposed method can keep the system stable with the system uncertainty.

The performance output $z(t)$, which is designed to be hover attitude, is denoted in Fig.9. From Fig.9, it can be seen that the

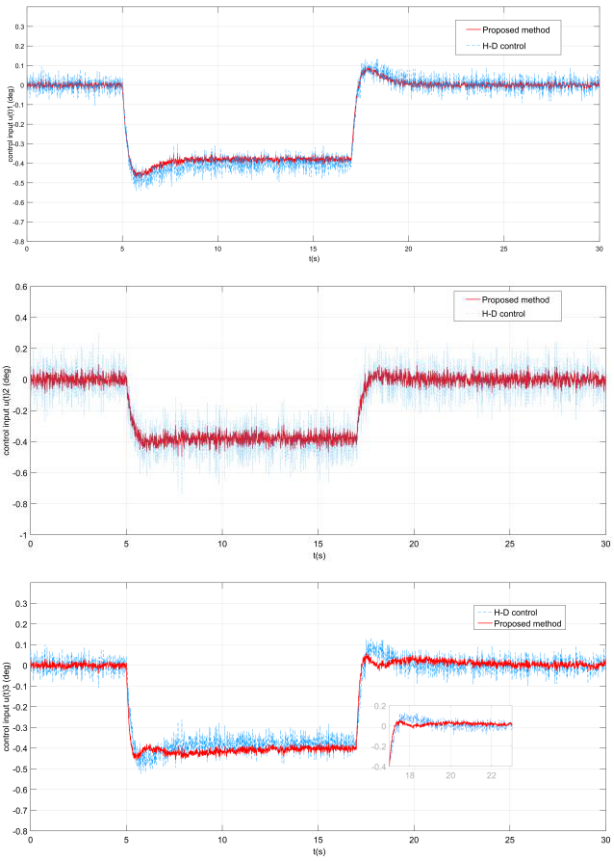

FIGURE 10. Control inputs of altitude response using H-D control and proposed method.

proposed observer-based controller stabilized the closed-loop system in the presence of disturbances, system uncertainty and sensor fault, and the effects of disturbance and fault on the performance output have also been weakened. The roll angle response and pitch angle response under the proposed controller converge to small neighborhood of zero in 4s, while the roll and pitch angle response under H-D control converge to small neighborhood of zero in almost 10s. In addition, the vibration amplitude of the proposed controlller is 40% of the H-D control method. Moreover, the yaw angle response under the proposed method is not affected by disturbance, uncertainty and the fault, while it still has slight effect under the H-D control. When a sensor fault occurs, the designed controller succeeded in minimizing the effect of fault on the UAV input-output relationship and ensuring certain level of robustness of the system output to noises and disturbances.

The comparison of the control inputs signals of the proposed method and the H-D control are presented in Fig. 10, which shows that the proposed method can achive faster convergence with smaller control effect. Also, it indicats that the control signals are continuos and physically realizable. The measurement noise in engineering is usually white noise, so we can get that the influence of disturbance and measurement noise on control performance and

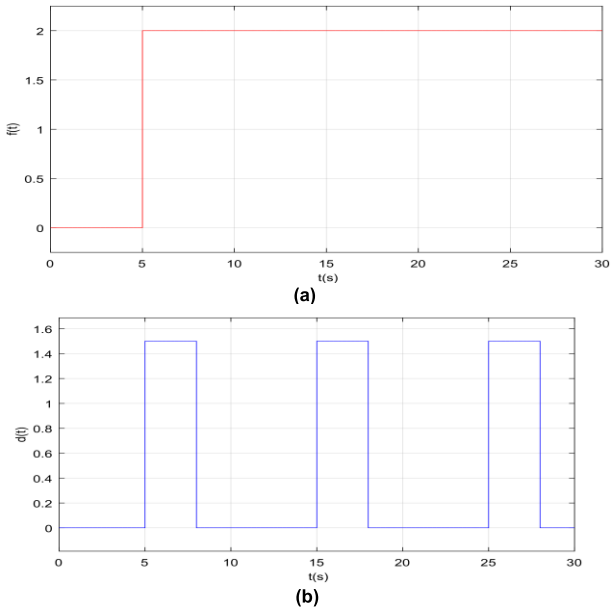

FIGURE 11. (a) Fault signal; (b) Disturbance signal.

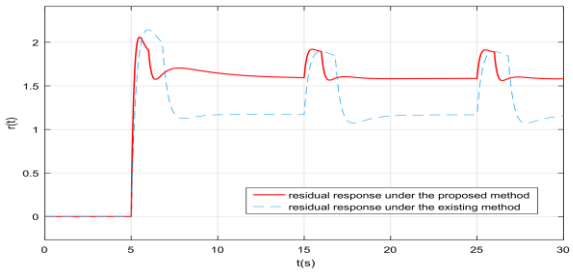

FIGURE 12. Residual response under the proposed method and residual response under the existing method.

input signal is weakened. Compared with the H-D control method, the proposed method has better noise and disturbances suppression effect, better robustness and easier engineering implementation.

C. FAULT ESTIMATION FOR LOW-FREQUENCY FAULT

To illustrate the effectiveness of the observer-based controller for the fault detection objectives, the fault and disturbance signals shown in Fig.11. The residual responses due to the proposed method in this paper and the exsiting method provided in [32] have been shown in Fig. 12. From Fig. 12 we can conclude that that the proposed observer-based controller has good fault sensitivity properties and good disturbance attenuation. Compared with the techniques which do not restrict the fault to a given specific frequency range, the effects of the low-frequency fault in residual are less susceptible to the disturbances effectes. Although the residual responses under the two methods are both affected by the disturbance, the proposed method in this paper has a better performance on fault detection and the control performance is also taken into account. However, due to the accurate description of fault frequency, the proposed method has some limitations in full frequency fault detection.

VI. CONCLUSION

This paper presented a solution to the simultaneous control and sensor fault detection problem for the ducted coaxial-rotor UAV in the presence of unknown disturbance and system uncertainties. A complete dynamic model has been established by analyzing the various forces and moments acting on the vehicle respectively. The control architecture was composed of an observer and a controller, which can achieve the fault detection objectives and control objectives simultaneously by one single unit in a design process. The major advantages of this article are as follows: 1) This design idea takes both control and fault detection objectives into account, and reduces the complexity of design. 2) The new approach can accurately characterize the finite frequency performance index by introducing the GKYP lemma to deal with the finite-frequency sensor fault detection problem. Through introducing a new form linearizing change-of-variables, the observer-based controller design conditions converted into LMI-based optimization problem. 3) Different from the most existing techniques, the proposed method is presented by a novel model, which contains time-varying system parameters uncertainty, then the LMI-based theorem can solve the fault tolerant problem with system uncertainty simultaneously. The simulation results have illustrated the proposed control design can guarantee the H_∞ performance to disturbance and system uncertainty, H_- performance which measured the fault sensitivity and stability of the closed-loop system.

The proposed method in this paper still has some limitations and can be improved in near future. Firstly, the method in this paper has some limitations in multi-fault detection and full-frequency fault detection. Second, some control performance may be lost while the detection performance is taken into account. Our future work will focus on fault tolerant control problem with multi-sensor faults and multi-actuator faults. In addition, simulation on nonlinear model and real flight tests should be performed.

REFERENCES

[1] K. Nonami, F. Kendoul, S. Suzuki, W. Wang, and D. Nakazawa, *Autonomous Flying Robots: Unmanned Aerial Vehicles and Micro Aerial Vehicles*. Heidelberg, Germany: Springer, 2010.

[2] D. Schafroth, C. Bermes, S. Bouabdallah, and R. Siegwart, "Modeling, system identification and robust control of a coaxial micro helicopter," *Control Eng. Pract.*, vol. 18, no. 7, pp. 700–711, 2010.

[3] E. N. Johnson and M. A. Turbe, "Modeling, control, and flight testing of a small-ducted fan aircraft," *J. Guid., Control, Dyn.*, vol. 29, no. 4, 2006, pp. 769–779.

[4] V. Duvvuri, "Modeling of an unmanned small coaxial helicopter," Ph.D. dissertation, Dept. Eng., Purdue Univ., Lafayette, Indiana, 2012.

[5] B. Xu, X. Wang, C. Xiang, Y. Ma, and W. Chen, "Modelling and hovering control of a novel multi-tandem ducted fan vehicle," in *Proc. Int. Conf. Unmanned Aircr. Syst. (ICUAS)*, Denver, CO, USA, Jun. 2015, pp. 9–12, doi: 10.1109/ICUAS.2015.7152429.

[6] P. Mukherjee and S. Waslander, "Modelling and multivariable control techniques for small coaxial helicopters," in *Proc. AIAA Guid., Navigat., Control Conf.*, Portland, OR, USA, Aug. 2011, pp. 8–11.

[7] H. Zhao, C. Bil, and B. Yoon, "Ducted fan VTOL UAV simulation in preliminary design," in *Proc. AIAA Aviation Technol., Integr., Oper. Conf. (ATIO)*, Hilton Head, CA, USA, Sep. 2009, pp. 21–23, doi: 10.2514/6.2009-7097.
[8] X. M. Yuan and J. H. Zhu, "Comprehensive modeling and analysis of an unmanned coaxial helicopter," in *Proc. AIAA Guid., Navigat., Control Conf.*, Kissimmee, FL, USA, Jan. 2015, pp. 5–9, doi: 10.2514/6.2015-0593.
[9] X. Chang, J. Huang, and F. Lu, "Robust in-flight sensor fault diagnostics for aircraft engine based on sliding mode observers," *Sensors*, vol. 17, no. 4, p. 835, 2017, doi: 10.3390/s17040835.
[10] S.-Y. Han, Y.-H. Chen, and G.-Y. Tang, "Sensor fault and delay tolerant control for networked control systems subject to external disturbances," *Sensors*, vol. 17, no. 4, p. 700, 2017, doi: 10.3390/s17040700.
[11] H. J. Kim and D. H. Shim, "A flight control system for aerial robots: Algorithms and experiments," *Control Eng. Pract.*, vol. 11, no. 12, pp. 1389–1400, 2003.
[12] J. M. Pflimlin, P. Souères, T. Hamel, and R. Mahony, "Position control and attitude stabilization of a Ducted fan VTOL UAV in crosswind," *IFAC Proc. Volumes*, vol. 39, no. 15, pp. 524–529, 2006.
[13] A. Drouot, E. Richard, and M. Boutayeb, "Nonlinear backstepping based trajectory tracking control of a gun launched micro aerial vehicle," in *Proc. AIAA Guid., Navigat., Control Conf.*, Minneapolis, MN, USA, Aug. 2012, pp. 13–16.
[14] M. R. Mokhtari, A. C. Braham, and B. Cherki, "Extended state observer based control for coaxial-rotor UAV," *ISA Trans.*, vol. 61, pp. 1–14, Mar. 2016.
[15] C. Spaulding, M. Mansur, M. Tischler, R. Hess, and J. Franklin, "Nonlinear inversion control for a ducted fan UAV," in *Proc. AIAA Atmos. Flight Mech. Conf. Exhibit.*, San Francisco, CA, USA, Aug. 2005, pp. 15–18, doi: 10.2514/6.2005-6231.
[16] R. Hess and M. Bakhtiari-Nejad, "Sliding mode control of a nonlinear, Ducted-fan, UAV model," in *Proc. AIAA Guid., Navigat., Control Conf. Exhibit.*, Keystone, CO, USA, Aug. 2006, pp. 21–24, doi: 10.2514/6.2006-6088.
[17] R. Aruneshwaran, S. Suresh, W. Jianliang, and T. K. Venugopalan, "Neural adaptive flight controller for ducted-fan UAV performing Nonlinear Maneuver," in *Proc. IEEE Symp. Comput. Intell. Secur. Defense Appl. (CISDA)*, Singapore, Apr. 2013, pp. 6–51.
[18] D. Nodland, H. Zargarzadeh, and S. Jagannathan, "Neural network-based optimal adaptive output feedback control of a helicopter UAV," *IEEE Trans. Neural Netw. Learn. Syst.*, vol. 24, no. 7, pp. 1061–1073, Jul. 2013.
[19] S. Zeghlache, H. Mekki, A. Bouguerra, and A. Djerioui, "Actuator fault tolerant control using adaptive RBFNN fuzzy sliding mode controller for coaxial octorotor UAV," *ISA Trans.*, vol. 80, pp. 267–278, Sep. 2018, doi: 10.1016/j.isatra.2018.06.003.
[20] X. Wang, C. Xiang, H. Najjaran, and B. Xu, "Robust adaptive fault-tolerant control of a tandem coaxial ducted fan aircraft with actuator saturation," *Chin. J. Aeronaut.*, vol. 31, no. 6, pp. 1298–1310, 2018.
[21] X. Zhang, Y. Zhang, C.-Y. Su, and Y. Feng, "Fault-tolerant control for quadrotor UAV via backstepping approach," in *Proc. 48th AIAA Aerosp. Sci. Meeting Including New Horizons Forum Aerosp. Exposit.*, Orlando, FL, USA, Jan. 2010, pp. 4–7, doi: 10.2514/6.2010-947.
[22] S. Mallavalli and A. Fekih, "Adaptive fault tolerant control design for actuator fault mitigation in quadrotor UAVs," in *Proc. IEEE Conf. Control Technol. Appl. (CCTA)*, Copenhagen, Denmark, Aug. 2018, pp. 193–198.
[23] M. Saied, B. Lussier, I. Fantoni, C. Francis, H. Shraim, and G. Sanahuja, "Fault diagnosis and fault-tolerant control strategy for rotor failure in an octorotor," in *Proc. IEEE Int. Conf. Robot. Autom. (ICRA)*, Seattle, WA, USA, May 2015, pp. 5266–5271.
[24] X. Wei and M. Verhaegen, "Mixed $H_{2212;}/H_\infty$ fault detection observer design for LPV systems," in *Proc. 47th IEEE Conf. Decis. Control*, Dec. 2008, pp. 1073–1078.
[25] S. Aouaouda, M. Chadli, P. Shi, and H. R. Karimi, "Discrete-time H_-/H_∞ sensor fault detection observer design for nonlinear systems with parameter uncertainty," *Int. J. Robust Nonlinear Control*, vol. 25, no. 3, pp. 339–361, 2015, doi: 10.1002/rnc.3089.
[26] J. Liu, J. L. Wang, and G.-H. Yang, "An LMI approach to minimum sensitivity analysis with application to fault detection," *Automatica*, vol. 41, no. 11, pp. 1995–2004, Nov. 2005.
[27] X. Wei and M. Verhaegen, "Mixed H_-/H_∞ dynamic observer design for fault detection," in *Proc. Eur. Control Conf.*, Budapest, Hungary, Aug. 2009, pp. 1913–1918.
[28] G.-H. Yang, H. Wang, and L. Xie, "Fault detection for output feedback control systems with actuator stuck faults: A steady-state-based approach," *Int. J. Robust Nonlinear Control*, vol. 20, no. 15, pp. 1739–1757, Oct. 2010.
[29] D. Henry and A. Zolghadri, "Design and analysis of robust residual generators for systems under feedback control," *Automatica*, vol. 41, no. 2, pp. 251–264, 2005.
[30] T. Iwasaki and S. Hara, "Dynamic output feedback synthesis with general frequency domain specifications," *IFAC Proc. Volumes*, vol. 38, no. 1, pp. 345–350, 2005.
[31] T. Iwasaki and S. Hara, "Generalized KYP Lemma: Unified frequency domain inequalities with design applications," *IEEE Trans. Autom. Control*, vol. 50, no. 1, pp. 41–59, Jan. 2005.
[32] A. Casavola, D. Famularo, and G. Franzè, "Robust fault detection of uncertain linear systems via quasi-LMIs," *Automatica*, vol. 44, pp. 289–295, Jan. 2008.
[33] X. Zhang, Y. Han, T. Bai, Y. H. Wei, and K. Ma, "H_∞ controller design using LMIs for high-speed underwater vehicles in presence of uncertainties and disturbances," *Ocean Eng.*, vol. 104, pp. 359–369, Aug. 2015.
[34] H. Wangm and G. H. Yang, "Simultaneous fault detection and control for uncertain linear discrete-time systems," *IET Control Theory Appl.*, vol. 3, no. 5, pp. 583–594, May 2009.
[35] M. R. Davoodi, H. Talebi, and H. R. Momeni, "A novel simultaneous fault detection and control approach based on dynamic observer," in *Proc. 18th The Int. Fed. Autom. Control (IFAC)*, Milano, Italy, Aug./Sep. 2011, pp. 12036–12041.
[36] M. R. Davoodi, N. Meskin, and K. Khorasani, "Simultaneous fault detection and control design for an autonomous unmanned underwater vehicle," in *Proc. IEEE GCC Conf. Exhibit.*, Doha, Qatar, Nov. 2013, pp. 17–20, doi: 10.1109/IEEEGCC.2013.6705835.
[37] A. R. S. Bramwell, G. T. S. Done, and D. Balmford, *Bramwell's Helicopter Dynamics*. London, U.K.: Heinemann, 2001.
[38] W. Xie, "Multi-objective H_∞ /α-stability controller synthesis of LTI systems," *IET Control Theory Appl.*, vol. 2, no. 1, pp. 51–55, 2008.
[39] W.-J. Mao and J. Chu, "Quadratic stability and stabilization of dynamic interval systems," *IEEE Trans. Autom. Control*, vol. 48, no. 6, pp. 1007–1012, Jun. 2003.
[40] S. Boyd, L. El Ghaoui, and V. Balakrishnan, *Linear Matrix Inequalities in System and Control Theory*. Philadelphia, PA, USA: SIAM, 1994.
[41] H. Wang and G.-H. Yang, "Integrated fault detection and control for LPV systems," *Int. J. Robust Nonlinear Control*, vol. 19, no. 3, pp. 341–363, 2009.
[42] C. Scherer, P. Gahinet, and M. Chilali, "Multiobjective output-feedback control via LMI optimization," *IEEE Trans. Autom. Control*, vol. 42, no. 7, pp. 896–911, Jul. 1997, doi: 10.1109/9.599969.
[43] L. Yu, *Robust Control-LMI Approach*. Beijing, China: Tsinghua Univ. Press, 2002.
[44] G.-L. Osorio-Gordillo, M. Darouach, L. Boutat-Baddas, and C. M. Astorga-Zaragoza, "H_∞ generalized dynamic observer-based control for uncertain descriptor systems," in *Proc. Amer. Control Conf.*, Boston, MA, USA, Jul. 2016, pp. 5644–5649, doi: 10.1109/ACC.2016.7526555.
[45] B. Xian and W. Hao, "Nonlinear robust fault-tolerant control of the tilt trirotor UAV under rear servo's stuck fault: Theory and experiments," *IEEE Trans. Ind. Informat.*, vol. 15, no. 4, pp. 2158–2166, Apr. 2019.
[46] D. Rotondo, A. Cristofaro, T. A. Johansen, F. Nejjari, and V. Puig, "Diagnosis of icing and actuator faults in UAVs using LPV unknown input observers," *J. Intell. Robot. Syst.*, vol. 91, pp. 651–665, Sep. 2018.
[47] K. Han, J. Feng, Y. Li, and S. Li, "Reduced-order simultaneous state and fault estimator based fault tolerant preview control for discrete-time linear time-invariant systems," *IET Control Theory Appl.*, vol. 12, no. 1, pp. 1601–1610, 2018.
[48] G. Ortiz-Torres, F. R. López-Estrada, J. Reyes-Reyes, C. D. García-Beltrán, and D. Theilliol, "An actuator fault detection and isolation method design for planar vertical take-off and landing unmanned aerial vehicle modelled as a qLPV system," *IFAC-PapersOnLine*, vol. 49, no. 5, pp. 272–277, 2016.
[49] F. R. López-Estrada, J.-C. Ponsart, D. Theilliol, Y. Zhang, and C.-M. Astorga-Zaragoza, "LPV model-based tracking control and robust sensor fault diagnosis for a quadrotor UAV," *J. Intell. Robot. Syst.*, vol. 84, nos. 1–4, pp. 163–177, Dec. 2016.
[50] R. Skelton, T. Iwazaki, and K. Grigoriadis, *A Unified Algebraic Approach to Linear Control Design*. London, U.K.: Taylor & Francis, 1998.

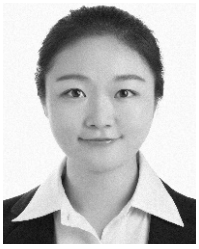

CHANG XU was born in Heilongjiang, China, in 1990. She received the B.S. degree from Northwestern Polytechnical University, Xi'an, China, in 2012. She is currently pursuing the Ph.D. degree with the Changchun Institute of Optics, Fine Mechanics and Physics, Chinese Academy of Sciences, Changchun, China. Her research interests include aircraft modeling, flight control, robust control, fault tolerant control, and failure detection.

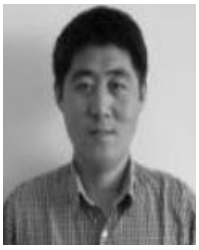

HONGGUANG JIA was born in Heilongjiang, China, in 1971. He received the B.S. degree from the Harbin Institute of Technology, Harbin, China, in 1994, and the M.S. degree from the Changchun Optical Engineering College, Changchun, China, in 1997, and the Ph.D. degree from the Changchun Institute of Optics, Fine Mechanics and Physics, Chinese Academy of Sciences, Changchun, in 2000. He is currently a Senior Researcher and Doctoral Supervisor with the Changchun Institute of Optics, Fine Mechanics and Physics, Chinese Academy of Sciences, Changchun. His research interests include combined guidance, flight control systems, electromechanical servo control technology, and the general design method of unmanned aerial vehicle.

ZAIBIN CHEN was born in Henan, China, in 1990. He received the B.S. degree from Sichuan University, China, in 2014. He is currently pursuing the Ph.D. degree with the Changchun Institute of Optics, Fine Mechanics and Physics, Chinese Academy of Sciences, Changchun, China. His research interests include flight control system design and digital imitation.